Proceedings of 46th Annual Review of Progression in Quantitative Nondestructive Evaluation
QNDE2019
July 14-19, 2019, Portland, OR, USA

QNDE2019-7055

ON THE USE OF THE GEOMETRIC MEDIAN IN ULTRASONIC ARRAY IMAGING

Nicolas Budyn*
Department of Mechanical Engineering
University of Bristol, UK

ABSTRACT

The standard and multi-view total focusing methods are increasingly popular ultrasonic array imaging techniques which post-process the full matrix array data by summing in-phase signals. This work proposes to replace the summation by the more robust geometric median to reduce the effect of detrimental high intensity signals, which is shown to result in artefact suppression.

Keywords: robust statistics, ultrasonic imaging, ultrasonic non-destructive testing.

1 INTRODUCTION

The total focusing method (TFM) [1] and the multi-view TFM [2] are increasingly popular ultrasonic array imaging techniques which post-process the full matrix array data by summing in-phase signals. Under this approach, the amplitude of an image point may be dramatically affected by the presence of a small number of high intensity signals such as wall echoes, resulting in large artefacts in the image. This paper proposes to replace the summation by the more robust geometric median to reduce the effect of these detrimental signals. This novel method removes the artefact from the image and recovers the signal of interest underneath, whilst leaving the uncontaminated area almost unaffected. Experimental results from the inspection of an aluminium block with a side-drilled hole are provided.

2 CONTEXT

Consider an ultrasonic array of N elements. The continuous-time signal transmitted by element i and recorded by element j is denoted $f_{ij}(t)$; it can be obtained from its discrete-time equivalent with any interpolation technique, such as Lanczos interpolation as used in this work [3]. A full matrix capture (FMC) consists in acquiring the N^2 time signals $\{f_{ij}(t) : i = 1..N, j = 1..N\}$. An image can be formed from the FMC data as a post-processing step using the total focusing method algorithm [1, 2]

$$I_0(\mathbf{r}) = \sum_{i=1}^{N}\sum_{j=1}^{N} \tilde{f}_{ij}(\tau_{ij}(\mathbf{r})), \tag{1}$$

where $|I_0(\mathbf{r})|$ is the pixel intensity at position $\mathbf{r}$, $\tilde{f}_{ij}(t)$ is the analytic (complex) signal obtained through the Hilbert transform, and $\tau_{ij}(\mathbf{r})$ is the time delay corresponding to the ray path from the transmitter i to the position $\mathbf{r}$ and finally to the receiver j. With the reduced notation $F_k = \tilde{f}_{ij}(\tau_{ij}(\mathbf{r}))$ with $k = i + Nj$ and with $n = N^2$, one can define

$$I_1(\mathbf{r}) = \frac{1}{n}\sum_{k=1}^{n} F_k. \tag{2}$$

$I_1(\mathbf{r})$ and $I_0(\mathbf{r})$ are equal up to a multiplicative factor $1/n$; as an image is generally rescaled by an arbitrary image point, this factor has no practical consequence. However, it becomes clear in Eq. (2) that $I_1(\mathbf{r})$ is the (complex) *arithmetical mean* of $\{F_k : k = 1..n\}$. Interpreting a complex number as a point in the complex plane, $I_1(\mathbf{r})$ is equivalently the *centroid* of the points $\{F_k : k = 1..n\}$.

Let us introduce a basic probabilistic model of the signal and the noise to justify the total focusing method. Interpreting the complex quantities as vectors of $\mathbb{R}^2$, let us assume the mea-

*Contact author: n.budyn@bristol.ac.uk

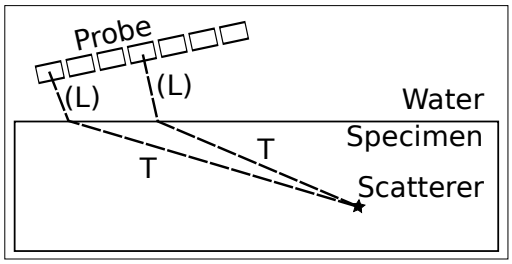

FIGURE 1: INSPECTION CONFIGURATION. THE SHOWN RAYS CORRESPOND TO THE VIEW T–T, WHERE *L* STANDS FOR LONGITUDINAL AND *T* FOR TRANSVERSE.

surements $\{F_k\}$ are normally distributed

$$F_k \sim \text{Norm}(\mu, \Sigma) \tag{3}$$

where μ is the signal of interest, $\mu \neq 0$ for a scatterer or $\mu = 0$ in the absence of a scatterer, and Σ is the 2×2 covariance matrix accounting for the grain noise. Assuming the $\{F_k\}$ are independent, then

$$I_1(\mathbf{r}) \sim \text{Norm}(\mu, \frac{1}{n}\Sigma) \tag{4}$$

which provides a theoretical signal-to-noise (SNR) enhancement of a factor n for TFM imaging. Remark: in practice, the SNR improvement is lower because the scatterer signal depends on the angles of insonification, i.e. $\mu = \mu_k$; we stick to the simpler model (3) as it is sufficient to illustrate our point.

The departure of $\{F_k\}$ from normality may have detrimental effects on the image. Consider the inspection configuration shown in Fig. 1 (detailed experimental apparatus given later). Figure 2a, the experimental TFM T–T image ($I_1(\mathbf{r})$) of the specimen, exhibits a large high-intensity artefact near location **A** created by the second reflection of the front wall. The wall echo has two essential properties: (i) its amplitude is significantly higher than the signal of interest μ, (ii) it overlaps with the scatterer in *some* but not *all* timetraces $f_{ij}(t)$ due to the geometry of the inspection. In other words, its time of arrival may or may not coincide with the time of arrival of the scatterer, therefore at a given point, the wall echo contaminates a limited number of points of $\{F_k\}$. To illustrate this, Fig. 3 shows $\{F_k\}$ at the scatterer-free image point **A**: most points are seemingly normally distributed around $(0,0)$, which corresponds to the grain noise, but some are significantly further away from the centre, which corresponds to the wall echo. The presence of these high-intensity signals has a dramatic effect on the centroid of the points $\{F_k\}$, which is as said previously the TFM result $I_1(\mathbf{r})$: the centroid is pushed away from the signal of interest $\mu = 0$ (Fig. 3b). This is an illustration of well-known lack of robustness of the arithmetical mean [4].

3 GEOMETRIC MEDIAN

As the mean of the signals used to form a TFM image is sensitive to outliers, we consider using the more statistically robust median instead [4]. In 1D, the (not necessarily unique) median m of a real-valued random variable X is such that $P(X \leq m) = 0.5$ and $P(X \geq m) = 0.5$, where $P(\cdot)$ denotes the probability. Equivalently, m is defined as

$$m = \underset{c \in \mathbb{R}}{\arg\min}\, E(|X - c|), \tag{5}$$

where $E(\cdot)$ denotes the expected value and c is the argument of the function to minimise. The geometric median extends the median in 2D [5]

$$m = \underset{c \in \mathbb{R}^2}{\arg\min}\, E(\|X - c\|_2), \tag{6}$$

where $\|\cdot\|_2$ denotes the Euclidean norm. A natural estimate of the geometric median of X using the independent and identically distributed samples $X_1, \ldots, X_n$ is

$$\hat{m} = \underset{c \in \mathbb{R}^2}{\arg\min} \sum_{k=1}^{n} \|X_k - c\|_2 . \tag{7}$$

Replacing the arithmetical mean by the geometric median in Eq. (2) leads to the new imaging algorithm

$$I_2(\mathbf{r}) = \underset{c \in \mathbb{R}^2}{\arg\min} \sum_{k=1}^{n} \|F_k - c\|_2 . \tag{8}$$

Geometrically, $I_2(\mathbf{r})$ is the point which minimises the sum of the Euclidean distances to the $\{F_k\}$. There is no closed formula for $I_2(\mathbf{r})$ in the general case (Fermat-Weber problem); however it can be calculated iteratively with Weiszfeld's algorithm [6, 7].

4 RESULTS

The inspection configuration is shown in Fig. 1. The 64-element 5-MHz ultrasonic linear array (pitch 0.3 mm) is held at a distance of 30 mm to the top surface and with an angle of 12°. The specimen is an aluminium block ($v_L = 4730\,\text{m}\,\text{s}^{-1}$, $v_T = 2280\,\text{m}\,\text{s}^{-1}$) with a side-drilled hole (SDH) of diameter 2 mm. Figure 2 shows the TFM images using respectively the mean and the median for the view T–T: the front wall artefact present in Fig. 2a is effectively removed by the use of the median in Fig. 2b, which makes the scatterer signal clearly visible. The rest of the image is unaffected, except minor changes near the wall echoes ($x \leq 20\,\text{mm}$), which is outside the area of interest. Figure 3 shows the geometric median of $\{F_k\}$ at point **A** is significantly closer to $(0,0)$ than the centroid, which explains why the artefact is removed.

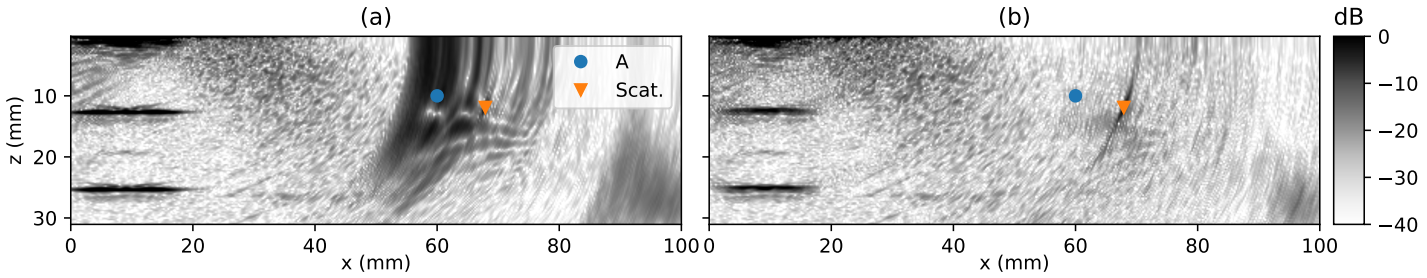

FIGURE 2: TFM VIEW T–T USING (a) THE ARITHMETICAL MEAN $I_1(\mathbf{r})$, (b) THE GEOMETRIC MEDIAN $I_2(\mathbf{r})$. POINT **A** IS PART OF THE ARTEFACT CAUSED BY THE SECOND FRONT WALL REFLECTION. THE IMAGES ARE ON THE SAME DECIBEL SCALE; 0 dB IS THE SCATTERER SIGNAL IN (b).

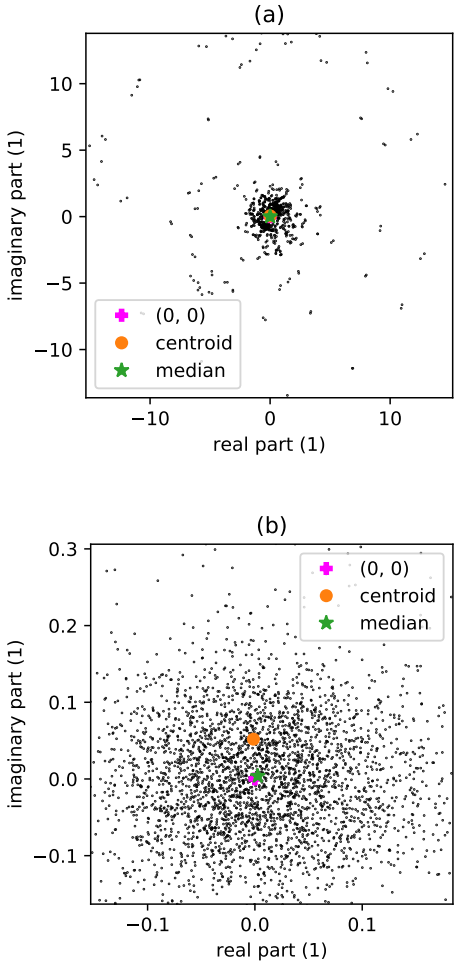

FIGURE 3: $\{F_k : k = 1..n\}$ AT POINT **A** FOR THE VIEW T–T. (a) FULL RANGE. (b) ZOOM IN.

ACKNOWLEDGMENT

This work was supported by the UK Research Centre in Non-Destructive Testing (RCNDE) [EPSRC grant EP/L022125/1] and BAE Systems. The author thanks Dr Rhodri Bevan for having provided the experimental dataset and Pr Anthony Croxford for his comments which greatly improved the manuscript.

REFERENCES

[1] Holmes, C., Drinkwater, B. W., and Wilcox, P. D., 2005. "Post-processing of the full matrix of ultrasonic transmit–receive array data for non-destructive evaluation". *NDT & E International,* **38**(8), pp. 701–711.

[2] Zhang, J., Drinkwater, B. W., Wilcox, P. D., and Hunter, A. J., 2010. "Defect detection using ultrasonic arrays: The multi-mode total focusing method". *NDT & E International,* **43**(2), Mar., pp. 123–133.

[3] Duchon, C. E., 1979. "Lanczos Filtering in One and Two Dimensions". *Journal of Applied Meteorology,* **18**(8), Aug., pp. 1016–1022.

[4] Maronna, R., Martin, D., and Yohai, V., 2006. *Robust Statistics: Theory and Methods*. Wiley Series in Probability and Statistics. Wiley.

[5] Kemperman, J., 1987. "The median of a finite measure on a Banach space". *Statistical data analysis based on the L1-norm and related methods (Neuchâtel, 1987)*, pp. 217–230.

[6] Weiszfeld, E., 1937. "Sur le point pour lequel la Somme des distances de n points donnés est minimum". *Tohoku Mathematical Journal, First Series,* **43**, pp. 355–386.

[7] Weiszfeld, E., and Plastria, F., 2009. "On the point for which the sum of the distances to n given points is minimum". *Annals of Operations Research,* **167**(1), Mar., pp. 7–41.